Metrology of Ultra-Lightweight X-Ray Optics Using Non-Contact Laser Triangulation Probe

Theo Hadjimichael[1], David Content[2], Charlie Fleetwood[1], Timo Saha[1],
Eugene Waluschka[2], Geraldine Wright[2]

1. Swales Aerospace, Beltsville, MD
2. Optics Branch, NASA Goddard Space Flight Center, Greenbelt, MD

1. Abstract

We are reporting our progress in the measurements of thin glass optics under development for the soft X-ray telescope for the Constellation-X space observatory. We are using a Non-Contact laser probe (which uses triangulation techniques to measure displacement) to determine the surface shape of our ultra-lightweight mirrors. If this technique meets technical specifications we will for the firs t time have mapped the 3 dimensional surfaces of ultra-lightweight optics. As a secondary project, we are also automating this entire process which will give us better repeatability.

2. Introduction

The noted success of the Chandra x-ray telescope underscores the growing astronomical interest in x-ray sources such as black holes, supernovae, galaxy clusters, etc. The Constellation-X follow-on mission now under development [1] aims to collect many more x-ray photons from each source so as to allow x-ray spectroscopy. Our aim is a highly sensitive soft x-ray space observatory (0.25-10 keV energy, or ~6 to 0.1 nm wavelength range). Each of 4 identical co-pointed telescopes will be comprised of many nested thin (0.4 mm) shells of grazing incidence mirrors. Our group is a part of collaboration between GSFC, MIT, MSFC, and SAO developing the technologies required to fabricate, test, assemble, and align these telescopes.

This paper is a progress report on efforts to measure the shape of these optics at various points in the fabrication process and to compare them to the mandrels used to make them. Details of the fabrication process are available elsewhere [2]. For purposes of this paper, consider the optics to be 60° segments of cones with diameter ~500mm, cone angle ~1° or less, and length 20 cm, 0.4 mm thick. This paper is a modification of a previous paper, it will give a brief overview of the test-bed in the lab and integration of separate components. A discussion on implementation of tests for the optics will be followed by our data analysis results and conclusions.

3. Explanation and Integration of CMM Components

At NASA Goddard Space Flight Center we have a Moore Coordinate Measuring Machine (MCMM), model number 3. The MCMM has a lateral (x and y) axis resolution of 0.5 micron and a vertical (z) axis, 2.54 microns, as a stand-alone instrument. X-axis range is 457mm, y 279mm, and z 432mm. The whole instrument is on air vibration isolation pads and in a semi temperature controlled room (± 1° C).

In order to achieve the required measurement accuracy, we had to modify our original Moore Coordinate Measurement Machine. An Axiom 2/20 Laser Measurement System, developed by Zygo, has been retrofitted to the MCMM, replacing the dial gauges for each of the three axes. The Axiom 2\20 uses a helium-neon laser to interferometerically measure linear displacement. By attaching optics and receivers to each axis, we are able to keep track of distance traveled to a much higher degree of accuracy than the original Moore X, Y, and Z dials; we can achieve a maximum nominal resolution of 1.25 nanometers, updated at 7 to 13 megahertz. This data is sent to a computer, which can provide a number of storage and data manipulation options. In practice the resolution repeatability is poorer than this, presumably in part due to the limited environmental control; the best measurement repeatability we can achieve is 200 nm rms.

We have recently mounted a non-contact probe to the MCMM. The Microtrak 7000 Laser Displacement Sensor with MT-100-5 Sensor Head developed by MTI Instruments, Inc. (see Fig 1) uses a small helium-neon laser and triangulation techniques to display surface displacements. It was originally intended to measure displacements across machined surfaces such as grooves, channels or step heights. We are using it to measure across a much larger and continuous range. It has a standoff distance of 25.4 mm, a resolution of 0.005 microns, and a linear range of 127 microns with a nominal spot size of 36 x 56 microns. When retrofitted to the Moore its function will be to take many measurements across an entire target optic in order to gain a 3-D map of its surface. The data from this controller is interfaced into a LabView computer program written at Swales Aerospace and coupled with the data from the Axiom 2/20 Laser Measurement System with multiple organizational and manipulation features.

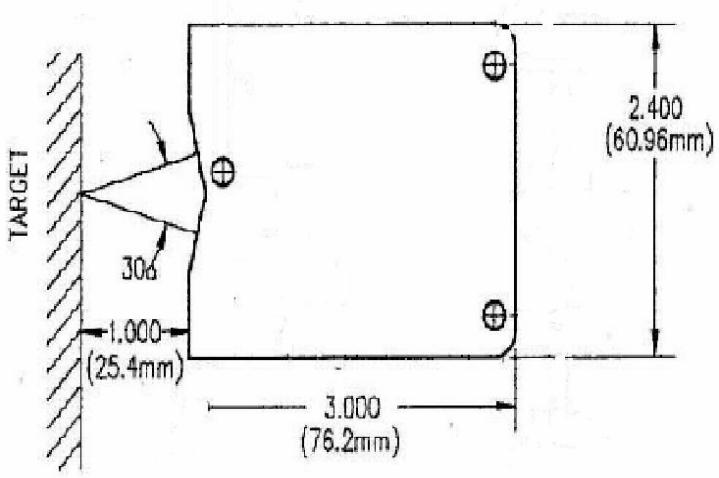

Figure 1: MTI Non-Contact Probe

The final components added to the MCMM are a set of Klinger stepper motor linear and rotation stages (see figure 2). In order to gain the proper in-plane motion, i.e. radial motion, of the part to be measured with respect to the probe, this extra linear stage had to be added on top of the circular stage. The Klinger stages were chosen so that we could easily automate our system. The automation of these stages was also incorporated into the LabView program. The linear stage has a nominal resolution of 0.1 microns and the circular stage a resolution of 0.001 degrees. To summarize the newly modified CMM, these two Klinger stages are mounted atop one another to the X-Y stage of the MCMM. The MTI non-contact probe is mounted to the Z axis of the MCMM and the travel of each axis is measured by the Axiom 2/20 (see Figure 1). Each of the devices are being kept track by a simple LabView code.

Figure 2: Moore CMM with non contact probe measuring large substrate on Klinger rotation and linear stages.

4. Initial Measurements

Initial tests of the system began on a diamond turned flat mirror. The alignment procedure was simple; the mirror is aligned parallel to the motion plane of the probe by aligning the mirror normal to the non-contact probe to within the probe's maximum displacement range in the x-z plane. A total of 413 points were recorded in a 15mm x 25mm square area. A least squares fit in MathCad was used to fit a plane to these points with a standard deviation, for the difference of the data and the fit, (hereafter rms) value of 1.9 microns. Although we know that the figure quality of this particular test flat is better than 0.1 micron RMS (measured by a WYKO interferometer) the value was sufficient to that needed for the x-ray mirror shape determination. We moved on with the ultimate goal to measure the Ultra-lightweight X-ray mirrors.

The next step was to try a 60 degree x 25 mm section of a diamond turned reference cone with a top radius of 89 mm and a half cone angle of 0.3 degrees. The part is known to be a straight right circular cone by virtue of its fabrication method and prior work on the MCMM and other metrology. Alignment of the

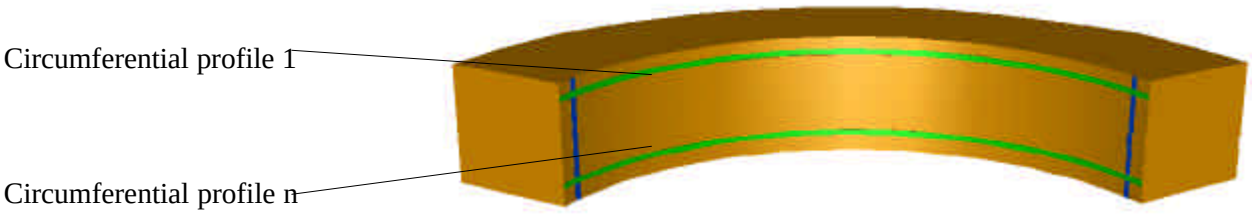

Figure 3: Aluminum reference cone with circumferential and axial paths outlined.

reference cone proved less simple along a curved surface as the non-contact probe becomes less reliable when trying to read at an incorrect incidence angle. We developed a process consisting of two stages: 1) mechanical alignment of the probe axis with respect to the axis of the rotation stage, and 2) iterative focus

adjustment of the part by scanning through the full 60° angular range at a given focus position to test whether the probe stayed in its limited range throughout the scan. This process was repeated until the full 60 degrees of the test part could be read (see figure 3. Note: circumferential profiles are 1 through n from top to bottom. In the data collection process the axial profiles, at every degree data was acquired, were a result of these 1 through n circumferential profiles). The LabView code could then be set to automatically take readings of all axes including rotation every x degrees for a total of 60 degrees and then return to its original position. As the Z-axis is not automated, at the end of each profile the z-axis is then moved to the next desired height (in the case of the reference cone every 1 mm) and the next circumferential profile is taken.

Once these measurements were acquired and the process was proven to work, a Constellation X substrate was placed against the alignment posts and a 3-D map of the surface was obtained. The substrates have a midpoint diameter of approximately 489 mm. Alignment of the cone to within the probes tolerances is fairly difficult. If the bisector of the probe triangulation beam is not aligned normal to the curved surface of the cone, a reading can still be gained traveling inside or outside of the designated 25 mm standoff distance, depending to which side the part curves with respect to the input pupil. Also the size of the surface (45-60° x 200mm) creates a problem such that as we move along the z-axis and rotate about a fixed radius, the probe is no longer able to stay within its 127 micron readable range. This is compensated for by subtracting the probe displacement measurements from x-axis measurements taken by the Axiom 2/20. Thus, when the probe is about to move out of its range the x-axis on the MCMM can compensate and bring the probe back to within the required 25.4±0.127 mm of the test part.

5. Data Analysis

The analysis of our data took part in two phases. First, raw axial and circumferential profile data were reduced using an Excel spreadsheet. Then using a combination of IDL and MathCad programming a 3-D rendering of the data points and a cone fitting routine were applied. Using Excel to fit the four sides of our data; a top and bottom circularity measurement and the two side axial measurements, we are able to both show good 2-D profiles and possible extraction of some information on how our part is misaligned. This misalignment analysis may allow us to retake our data for a better dataset with less error. The results of this data reduction are shown in Table 1 and Figures 4 and 5.

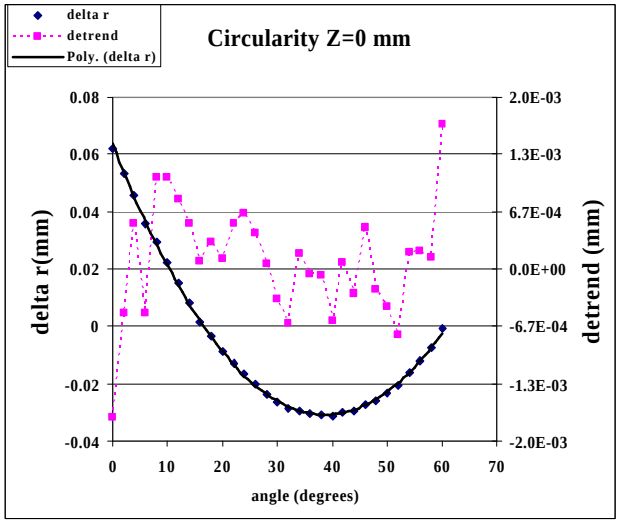

Figure 4: Circumferential profile reference cone, 2nd order fit

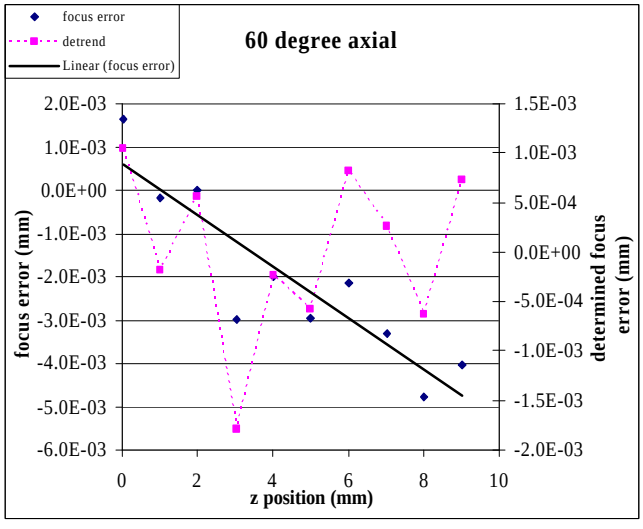

Figure 5: axial profile of reference cone, first order (tilt) removed

In both figures small diamonds represent the raw displacement data while the large triangles represent the subtracted data from the fitted curve. Preliminary repeatability tests on the axial and circularity profile of the reference cone appear adequate but more analysis needs to be done in order to confirm exactly how well it repeated. For each of the circularity measurements we are seeing rms values from 0.6 to 0.8 microns and for axial measurements approximately 1.3 micron. The axial measurements fit to first order lines gave rms values of 0.8 to 1.6 micron (see table 1).

This same approach was then taken for the larger Constellation –X ultra-lightweight substrate mirrors. Again the axial measurements show rms values of 7 to 15 microns and circularity measurements of 2 to 3 microns (see table 1). The repeatability on the large substrate is harder to discern than with the reference cone. From a purely graphical standpoint the axial repeatability is poor while the repeatability on the circularity looks good. This may be a result of the much larger axial distance traversed on the large substrate, 100 mm, than on the reference cone, 9 mm. It will be necessary in the future to modify the test to take into account the changing radius as the height is traversed rather than compensating for the fact that the probe goes out of range by simply moving the test part closer and not changing the radius about which it rotates. This approach was fine for the reference cone as its change in radius with changing height remained in range of the non-contact probe.

		0° axial RMS(microns)	**60° axial RMS(microns)**
reference cone	test 1	1.6	0.9
	test 2	1.34	0.86
489s-90 Substrate	test 1	8.14	7.09
	test 2	2.64	2.56
		Z=0mm circularity RMS(microns)	**Z=9(100) circularity RMS(microns)**
reference cone	test 1	0.65	0.71
	test 2	0.65	0.79
489s-90 Substrate	test 1	2.65	3.2
	test 2	13.06	14.86

Table 1: Axial and Circumferential RMS values, in microns, of the reference cone and substrate.

In the next step in data reduction the raw data from the non-contact probe and Axiom 2/20 interferometer displacement devices were reconstructed from a Cylindrical (? ?, ?, Z) into a Cartesian coordinate system (X, Y, Z). This was accomplished by the addition of a nominal radius given by the known midpoint radius of the part in the case of the reference cone. For the case of the substrates the known mandrel midpoint radius, from which they were replicated, was used. This new Cartesian dataset was then brought into MathCad for reduction and graphic display. In each case we used a least squares method to fit the data. We used an iterative approach: 1) Allowing the dataset to move with 6 degrees of

freedom (representing small remaining misalignments) in order to find its best fit to the known, fixed mandrel (reference) cone formula. This removes any misalignment of the dataset to the fixed coordinate system. Typical angular and linear misalignments were on the order of 0.2 degrees and 0.2 mm respectively. 2) The actual best fit cone was found again using a least squares approach and a comparison of known to actual cone formulas was made. The results of this hierarchical approach are summarized below (see table 2).

		Reference Cone test 1	Reference Cone Test 2	Substrate 489s-90 test 1	Substrate 489s-90 test 2
Measured Values	**half-cone angle(degrees)**	**0.323**	**0.5201**	**1.71**	**1.91**
	Initial Radius (mm)	**89.23**	**89.21**	**243.72**	**244.05**
	RMS (microns)	**1.8**	**2.4**	**8.3**	**6.64**
Mandrel Values	**half-cone angle(degrees)**	**0.3**	**0.3**	**0.96**	**0.96**
	Initial Radius (mm)	**88.9**	**88.9**	**243.997**	**243.997**

Table 2: Final MathCad test results and Comparison for Substrate and Reference Cone

6. Continued Work

After close examination of the previous data it was decided to better classify the non-contact probe with respect to our other means of metrology. Comparisons against a contact probe and a Wyko interferometer were then made. A preliminary test was made on a large glass forming mandrel. This sort of testing with[3] a contact probe we are very familiar with. The idea was to take a step backwards and use a test where the traditional contact probe is a sufficient measurement tool and compare it against how well the non-contact probe performs on the same part. The mandrel tested is referenced by a 229 mm diameter and 208mm high with 16.7 mm thick walls. The surface measurements were of the outside wall i.e. a convex surface with respect to the probe as apposed to the concave surfaces previously read on the Constellation-X Ultra-lightweight optics. A full 360° profile was taken with each probe twice and at the same height every 10°. Unlike previous measurements the mandrel was placed on a large, ultra-stable rotation stage associated with the Moore Coordinate Measuring Machine. This stage is not an automated stage therefore was not used in previous test configurations. The results

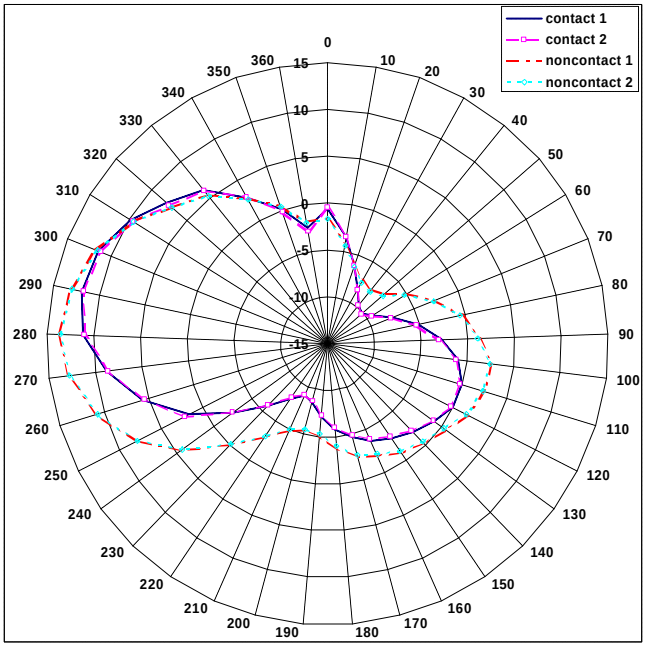

Figure 6: Mandrel data, contact versus non contact

of this test are promising (see figure 6). The curves of the non-contact and contact probes are repeatable (rms values 0.07 microns and 0.16 microns respectively). The two different probes also agree with each other to approximately 3 microns.

The next step was to return to the aluminum, diamond turned reference cone (see fig. 3). The same test was repeated on this aluminum mandrel 60° section as was accomplished for the forming mandrel explained above. The differences between the two tests are: 1) concave versus convex surface with respect to the probe. 2) Aluminum versus Glass (different reflectivity) 3) Alignment process much harder when not attempting a full 360° part. The first two points are made in reference to how much light is returned to the probe. The last point is made simply because misalignment can be a rather large factor in data reduction. What was determined from the results was somewhat shocking. It can be seen from figure 7 that the non-contact probe and the contact probe while separately repeatable have much different noise levels. Where in the previous test on the large forming mandrel each curve was smooth the plotted data from the non-contact probe measuring the aluminum reference cone section has a measurable noise level of approximately 1 micron. The non-contact probe measured noise is approximately 0.2 microns. On the other hand the repeatabilities are 0.2 and 0.07 microns respectively. These repeatabilities agree with those acquired from tests on the forming mandrel described above.

Figure 7: plots of Contact and Non-Contact detrends from glass mandrel

Noting that the non-contact data plot looked relatively sinusoidal the next test was devised in order to better understand the noise in the system and possibly determine why it was repeatable. Moving onto a small substrate the same test was again repeated. This time four profiles were taken at the same height. Each profile, however, was taken with different step angles; 2°, 1.5°, 1°, and 0.5° (see figure 8). Again we see high repeatability as well as high noise values agreeing with the previous test. This seems to lean away from possible explanations for high noise level such as reflectivity or type of material. We still have to look at the possibility of shape being a strong factor. In other words how do the probes differ between readings a concave versus convex versus flat (which we have as yet to look into).

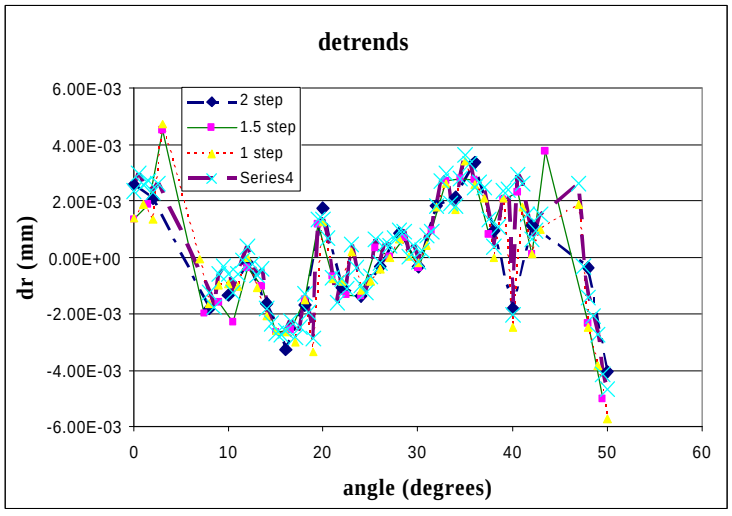

Figure 8: detrend plots of four profiles on aluminum reference cone (same height).

6. Conclusion

Our results from our upgraded non-contact mode Moore CMM look promising. Some modifications still need to be made in our data taking procedure. For instance, on larger parts, allowing the radius to change with changing height and recording this change into our final LabView dataset. Also the least squares data reduction and hierarchic approach is possibly too simple. Looking at the results of this data reduction it seems that we are falling into local minima where the radius seems to be finding a close fit, but the half cone angles are evidently not well fit. We are looking into Global fitting techniques in order to correct for this. Finally we are moving towards a fully automated system in which not only will the Z-axis automated but our LabView code will be programmed to compensate for known radius changes and to be able to recognize when the non-contact probe is out of range and compensate appropriately. More work still needs to be done in our probe classification. We are looking into different non-contact technologies that may give better noise results while keeping the good repeatability numbers.

Acknowledgements

David Colella, Mantec; Tammy Faulkner, Swales Aerospace; Tim Mengers, Swales Aerospace
Disclaimer: Mention of trade names or commercial products does not constitute endorsement or recommendation by NASA or by Swales Aerospace.

References

[1] See the description of Constellation-X online at http://constellation.gsfc.nasa.gov/
[2] W. W. Zhang, K. Chan, D. A. Content, R. Petre, P. J. Serlemitsos, T. T. Saha, Y. Soong, "Development of mirror segments for the Constellation-X Observatory," Proc. SPIE **4851**-58 (2002).
[3] D. A. Content, D. Colella, C. Fleetwood, T. Hadjimichael, T. Saha, G. Wright, W. Zhang, "Optical metrology for the segmented optics on the Constellation-X soft x-ray telescope," Proc. SPIE [5168-23] (2003).